

Juho Pirttilahti, Sakari Pollari, Janne Kapela

Safety system delay measurement and implementation to VR- simulation

Keywords: delay, stopping time measurement, virtual reality, safety validation, digital twin

Pirttilahti, Juho: Seinäjoki University of Applied Sciences, juho.pirttilahti@seamk.fi

Pollari, Sakari: Seinäjoki University of Applied Sciences, sakari.pollari@seamk.fi

Kapela, Janne: Seinäjoki University of Applied Sciences, janne.kapela@seamk.fi

Abstract

This paper examines the distinctions between virtual and real-world environments in the assessment of machine safety applications. The high-speed camera was employed for the actual configuration for measurement of a single DC motor stop time, which represents part of the real machine architecture. The delay between the activation of the safety laser scanner and the cessation of the motor was measured. Additionally, the delay from the safety laser scanner to the contactor shut down operation was measured. The result serves to establish a benchmark for comparison with a virtual model developed in Unity.

The virtual environment is constructed in such a way as to replicate the real-world system, with the objective of implementing real-world measured delay and safety performance under controlled conditions. By simulating different scenarios, researchers can assess the system's response and identify critical weaknesses without the inherent risks associated with physical machinery.

Latency is a critical factor in the context of safety. It is defined as the time interval between the triggering of a safety condition and the corresponding system action. The reduction of latency is of paramount importance for the implementation of effective safety responses. In the virtual setup, computational latency is analyzed in conjunction with real-world mechanical delays to ascertain the viability of utilizing virtual simulations for safety-critical assessments.

Moreover, the study assesses compliance with ISO 13849-1, a foundational safety standard that delineates the specifications for control system design. Verification of adherence to these criteria in both the virtual and physical setups serves to validate the robustness of simulations for machine safety systems. The integration of high-speed camera data improves the accuracy of the virtual model, enabling a comprehensive analysis of system behavior under dynamic conditions.

Introduction

In machine safeguarding, time delay in a safety system's response can be the difference between a near miss and severe injury. ISO 13849-1 standard [1] highlights that the safety function design must consider the machine's stopping performance. The delay is a crucial factor when a person or object approach dangerous parts of the machine. From this view, the B1-type standard ISO 13855 [2] is constructed to include the calculation of safety distances. The standard introduces Formula 1 for separation distance.

$$S = K \times T + D_{DS} + Z$$

Formula 1: Separation distance calculation according to ISO 13855

Here K is the assumed approach speed of the body or body part, T is the overall system response time, D_{DS} is the reaching distance associated with the protective device and Z is the additional distance constant determined by the application, which is more commonly referred to as safety margin [2]. From this formula, because S scales with T , even small increases in delay can demand significantly large safety distances. If we assume that quick movement of the hand could be done with the speed of 2000 mm/s, the additional delay of one second would require about 2000mm more separation distance to the dangerous parts of the machine. This translates to 2 mm more separation distance for every millisecond of additional delay introduced by the safety system.

Integrating virtual reality into machine system development offers a transformative methodology for system evaluation and verification, particularly in relation to safety and operational efficacy. By employing VR technology, comprehensive testing of both functionality and safety features can be conducted prior to physical deployment, thereby mitigating risks, and reducing development costs [3]. In VR, designers can simulate real-world conditions with high precision. For instance, VR can replicate the dynamics of machine tools, such as lathes and milling machines, allowing designers to evaluate various scenarios, including different speeds and separation distances, to identify potential hazards [4][5]. This capability is particularly useful for evaluating the safety of automatically controlled machine tools, where human-machine interaction is critical [4]. However, while VR offers substantial benefits for safety validation, there is a risk of learning false information if simulations do not adequately cover all safety aspects or reflect real-world parameters [6].

Methodology

To replicate key aspects of the actual machine architecture, a real-world experimental setup was constructed. The test environment was intended to serve as a reference for the virtual model to be created and to utilize the measurement data obtained from it to create the most accurate digital twin possible.

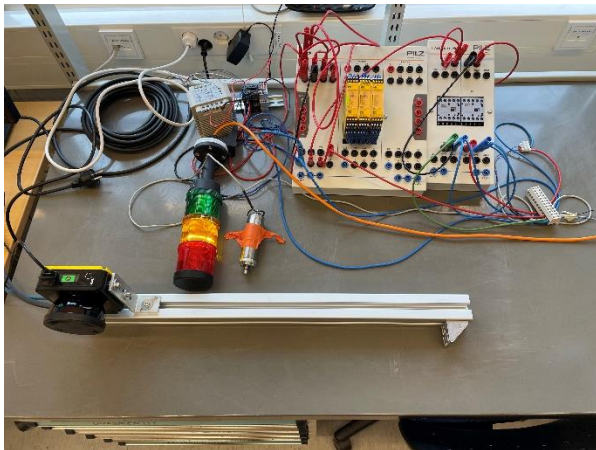


Figure 1: Test setup consisting of the components for safety architecture.

In the wiring of the safety laser scanner, the example provided in the Pilz PNOZ S4 operating instructions [7] for connecting the OSSD outputs to the safety relay was used. The test setup is shown in Figure 1. The safety laser scanner’s OSSD1 and OSSD2 outputs are connected to the Pilz PNOZ S4 safety relay’s S12 and S22 connectors. The safety relay’s outputs, terminals 13–14 and 23–24, control the motor’s front contactors

K1 and K2. The supply voltage to the motor passes through terminals 13–14 of the K1 and K2 contactors, forming a series connection for the motor’s supply. This configuration creates a category 0 stop by disconnecting the motor’s power supply. More detailed electrical drawings are shown in Figure 2.

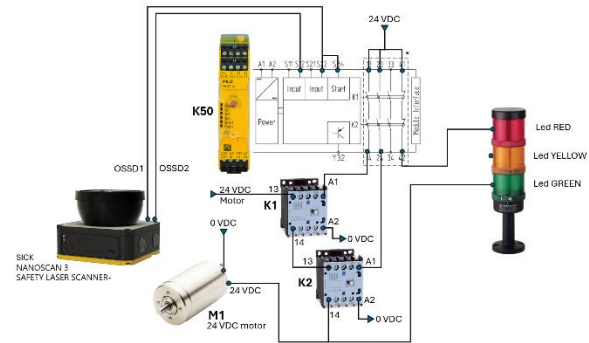


Figure 2: Electrical schematics of test setup.

Delay measurements were performed using a Citius Imaging C100 high-speed camera in conjunction with Citius Imaging 1.48 software, which was configured to capture images at intervals of 2.306 milliseconds. The safety laser scanner (Sick nanoScan3), configured with a 20 mm finger detection resolution, was mounted vertically on an aluminum profile bar, and aligned with the camera to ensure reliable observation of the safety field activation [8]. The verification report, which shows the area of the laser scanner is shown in Figure 3.

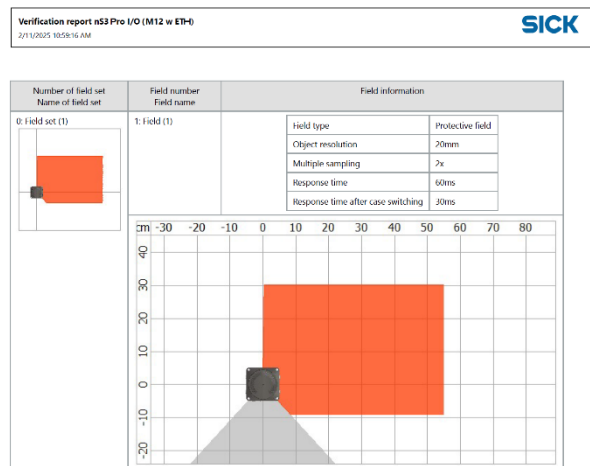


Figure 3: Verification report of protective field information.

The camera’s field of view also encompassed a small DC motor equipped with a mechanical rotation indicator and signal lights. These lights indicated the activation of the safety relay (Pilz PNOZ s4) and the switching of the contactor. For the experiment, an operator’s hand was employed to trigger the safety light curtain, and the subsequent video recordings were analyzed—using the

known frame rate—to calculate the delay from safety field activation to motor cessation. The visualisation of the high-speed camera picture is shown in Figure 4.

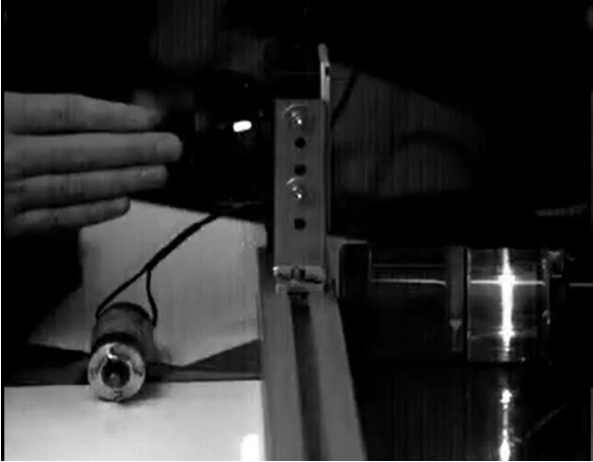


Figure 4: Screenshot from highspeed camera video taken from test setup.

According to manufacturers' datasheets, the configuration introduces a minimum switching delay of 70 ms for the Sick nanoScan3 [8]. The Pilz PNOZ S4 safety relay exhibits a switch-off time of 10 ms [7]. The WEG CWC016 motor contactor has a contact opening time ranging from 7 to 12 ms when operated by a 24 VDC coil [9]. Together, these components result in a total stopping time ranging from 87 ms to 92 ms. The motor itself does not have a defined nominal stopping value, and significant variation was observed during testing.

After the real-world measurements, a virtual reality (VR) model of the test setup machine and its safety control system was developed in Unity. This VR model replicated the stopping architecture of the physical system, with delays for each component (safety light curtain, safety relay, contactor, and motor) parameterized based on the high-speed camera data. The Unity object code was modified to incorporate the motor's ramp-down time, and parameters encompassed an error margin ranging from 1 millisecond to 1 second. This was included in the test using a random generator to emulate a similar standard deviation effect observed in real-world tests.

Constructing the VR Environment

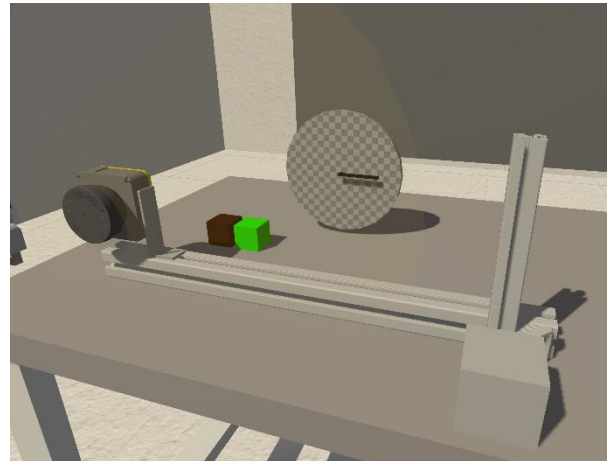


Figure 5: Test setup replicated in VR.

The VR simulation was built to mirror the real machine's safety system, including a virtual curtain, relays, and the motor stop sequence. The test setup is visualized in Figure 5. The light curtain in VR is represented by an invisible sensor zone that detects intrusions just like a physical light curtain would. In the real system, breaking a light curtain's beams immediately triggers a safety response: the light curtain's outputs turn off and the safety relay cuts power to the motor, bringing hazardous motion to a stop [10]. The VR model replicates this chain of events. When the user (or any object) crosses the virtual light curtain's plane, the simulation initiates an emergency-stop routine that sequentially emulates the relay activation and motor braking, just as the real hardware would. By reproducing each component's function and interaction, the VR setup acts as a digital twin of the safety system, ensuring that the virtual machinery responds to safety breaches exactly like the real machinery.

The simulation does not immediately stop the machine upon intrusion to reflect real safety system timing. Instead, it introduces staged delays that correspond to each component's reaction time. This was accomplished in Unity by using sequential timed events to represent the delay at each step of the safety chain. For example, when the virtual light curtain is breached, an initial trigger fires and starts a short countdown representing the light curtain's detection and processing time. Once this delay elapses, the next step simulates the safety relay's response – after its own configured delay, it “opens” the circuit in the simulation.

Finally, after the relay delay, the motor stop sequence is executed: the VR motor begins decelerating or

halting over an additional brief period to imitate the motor's coast-down time. Each timed step in the simulation is governed by an adjustable response parameter, allowing the delay between stages to be fine-tuned to match the exact milliseconds observed in real-world measurements. In addition, an adjustable error margin parameter is incorporated to simulate the inherent measurement errors and natural variability seen during physical testing. This dual-parameter approach effectively strings together the sequential delayed reactions—from sensor activation, through relay switching to motor stopping—recreating the cascade of events in an actual emergency stop. By calibrating both the nominal delays and their associated error margins, it is ensured that the overall stop time in VR not only aligns closely with reality but also reflects its dynamic variability. The setup values are introduced in Figure 6.

Settings			Error	
Sensor Delay	0.10	TYPE	0.05	TYPE
Relay Delay	0.10	TYPE	0.05	TYPE
Tool Delay	0.10	TYPE	0.05	TYPE
Tool Slowing	0.50	TYPE	0.05	TYPE

Figure 6: Delay parameters and error parameters for deviation.

Why parameterize these delays? In a real safety circuit, each device introduces a known reaction time. Manufacturers of safety components specify how quickly their device responds – for instance, a light curtain might have a response time of tens of milliseconds, and a safety relay might add its own small delay (often in the 10–40 ms range) [11]. In the VR model, these times are not hard coded as fixed values; instead, they are exposed as parameters that can be configured. This approach allows users to plug in the exact timings from the device datasheets (or from empirical measurements) for each component. It also makes the simulation flexible: if a different sensor or relay is used in the future (with a different spec), or if the real system's performance is re-measured, the virtual model can be updated by simply changing the delay parameters. In short, parameterizing the delays ties the simulation's behavior directly to manufacturer-specified values, which is essential for realism [11]. According to safety standards, the response time of the presence-sensing device as stated by the manufacturer or measured by the employer must be accounted for in

safety calculations – the VR follows this principle by using those same values in the model. The VR- setting with test scoreboard is illustrated in Figure 7.

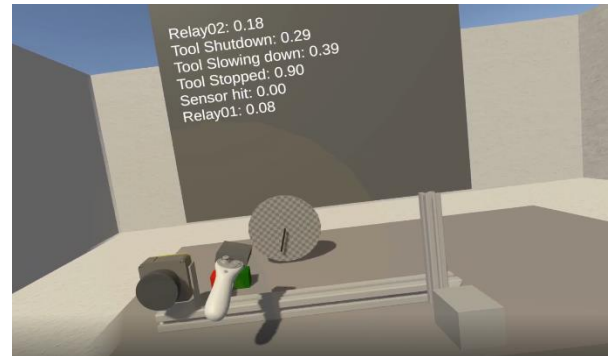


Figure 7: VR- test setting with delay time scoreboard.

Results and Discussion

The high-speed camera system was employed to conduct two distinct measurement configurations. In the first measurement, the delay from the activation of the safety scanner to the cessation of the motor was evaluated. This test was repeated ten times, yielding a mean delay of 1404.79 ms with a standard deviation of 50.12 ms.

In the second configuration, indicator lights were incorporated into the circuit following the safety relay and motor contactor. These lights visually indicated the activation of the respective components, which were captured by the high-speed camera. The results from this setup revealed a mean delay of 14.87 ms with a standard deviation of 16.08 ms for the time between the activation of the safety sensor and the triggering of the safety relay. Additionally, the mean delay from safety scanner activation to the state change of the contactor was found to be 26.20 ms, with a standard deviation of 16.63 ms. This was found to be significantly faster than the delay calculated from the components' datasheets including the deviation. The total delay from the activation of the safety laser scanner to the cessation of the motor in this second setup was 1388.74 ms, with a standard deviation of 66.68 ms. When combining the results from all 20 trials, the total mean delay from the activation of the safety scanner to the cessation of the motor was 1396.77 ms, with an overall standard deviation of 61.10 ms.

The largest portion of the delay arises from mechanical deceleration of the motor rather than from the electronic or sensing components. The brief intervals measured between the scanner activation and the safety relay (~15 ms) or contactor off (~26 ms) are minimal in comparison. This is consistent with typical small motor inertia and the absence of an electronic brake in the test setup.

The short delays (e.g., scanner-to-relay or scanner-to-contactor) exhibit higher standard deviations (about 16 ms) compared to their mean values. This reflects the frame-based measurement resolution of the high-speed camera and potential jitter in signal switching. While the camera provides accurate timing over the full 1.40 s window, sub-30 ms intervals are proportionally more affected by each frame's ~2.36 ms increment.

Conclusions

The experimental results indicate that the high-speed camera reliably detected the laser light emitted by the safety scanner, thereby facilitating precise alignment during testing. However, further investigation is required to refine the accuracy of motor cessation event timestamp extraction from the video frames, as the software-based frame measurements exhibit a non-negligible tolerance.

In developing the virtual reality (VR) model, it was essential to parameterize two key factors: the nominal delay associated with each component and the additional delay introduced by measurement tolerance. This approach enables simulation of safety responses under various conditions, providing a robust framework for analyzing system behavior. Moreover, the VR environment allows for rapid testing and optimization of safety measures without the inherent risks and costs of physical trials.

The high-speed camera proved to be an effective tool for validating total delay times—from safety scanner activation to motor cessation—under conditions where safety tolerance is critical. Nonetheless, its precision diminishes when capturing noticeably short time intervals, such as those between the activation of the safety scanner and subsequent events like safety relay or contactor switching. Furthermore, while manufacturers typically provide component reaction times and delay values that incorporate built-in safety factors for practical applications, additional optimization may be necessary to reflect the dynamic performance of the system more accurately under test. However, based on the test, it is more feasible to inspect the stopping time of mechanical systems rather than electrical control systems.

Acknowledgements

The authors would like to thank the funder Regional Council of Southern Ostrobothnia for funding projects IXFactory development project (J10444) and ROHITVA - Robotic welding techniques in manufacturing SMEs (R-01026) where this application was first constructed and developed further. The article is co-funded by the

European Union. The logo is represented in Figure 8.



Figure 8 8: Funder logo.

Bibliography

- [1] International Organization for Standardization. (2015). *ISO 13849-1:2015: Safety of machinery—Safety-related parts of control systems—Part 1: General principles for design*. International Organization for Standardization.
- [2] International Organization for Standardization. (2010). *ISO 13855:2010: Safety of machinery—Positioning of safeguards with respect to the approach speeds of parts of the human body*. International Organization for Standardization.
- [3] Holubek, R., Delgado Sobrino, D. R., & Matúšová, M. (2024). *A new approach for creating and testing safety components integrated into a robotic cell simulation scenario in a virtual reality environment*. *Journal of Physics: Conference Series*, 2927, 012002. <https://doi.org/10.1088/1742-6596/2927/1/012002>
- [4] Herpers, R., Scherfgen, D., Vieth, M., Saitov, T., Felsner, S., Hofhammer, T., Schaefer, M., & Huelke, M. (2013). Vr-Based Safety Evaluation of Automatically Controlled Machine Tools. *International Conference on Games and Virtual Worlds for Serious Applications*, 1–4. <https://doi.org/10.1109/VIS-GAMES.2013.6624248>
- [5] Määttä, T. (2007). Virtual environments in machinery safety analysis and participatory ergonomics. *Human Factors and Ergonomics in Manufacturing & Service Industries*, 17(5), 435–443. <https://doi.org/10.1002/HFM.20084>
- [6] M. P. Jelonek, E. Fiala, T. Hermanns, J. Teizer, S. Embers, M. König, and A. Mathis, "Evaluating Virtual Reality Simulations for Construction Safety Training," *I-Com*, vol. 21, no. 2, pp. 269–281, 2022, doi:10.1515/icom-2022-0006.
- [7] Pilz GmbH & Co. KG. (n.d.). *PNOZ s4 operating manual* (Version 18, Document No. 21396-EN-18). https://www.pilz.com/download/open/PNOZ_s4_Operat_Man_21396-EN-18.pdf
- [8] SICK AG. (n.d.). *NANOSCAN3 I/O operating instructions* (Document No. IM0087137). https://cdn.sick.com/media/docs/7/37/137/operating_instructions_nanoscan3_i_o_en_im0087137.pdf

[9] WEG. (n.d.). WEG compact contactors – CWC0 series [PDF, p. 24]. WEG. <https://static.weg.net/medias/downloadcenter/h3d/h58/WEG-compact-contactors-CWC0-50069462-en.pdf>

[10] Rockwell Automation. (n.d.). Safety AT065 [PDF, p. 5]. Rockwell Automation. https://literature.rockwellautomation.com/idc/groups/literature/documents/at/safety-at065_-en-p.pdf

[11] Pinnacle Systems. (n.d.). *Safety distance light curtains*. <https://pinnaclesystems.com/safety-distance-light-curtains/#:~:text=Tc%20%3D%20Response%20time%20of,monitor%20to%20compensate%20for%20variations>